

Topology optimization of fluid channels with flow rate equality constraints

Zhenyu Liu · Qingyong Gao · Ping Zhang ·
Ming Xuan · Yihui Wu

Received: 19 May 2010 / Revised: 6 October 2010 / Accepted: 16 October 2010 / Published online: 16 November 2010
© Springer-Verlag 2010

Abstract This note presents topology optimization of fluid channels with flow rate equality constraints. The equality constraints on the specified boundaries are implemented using the lumped Lagrange multiplier method. The quadratic penalty term and cut-off sensitivity are used to maintain the stability of optimization.

Keywords Topology optimization · Navier–Stokes equation · Equality constraint · Lagrange multiplier

1 Introduction

Layout optimization of fluid channels is an important topic when designing microfluidic devices (Okkels et al. 2005; Okkels and Bruus 2007; Andreasen et al. 2008; Deng et al. 2010; Takagi et al. 2005; Vangelooven et al. 2010). Usually, layout optimization can be categorized into either shape or topology optimization. Shape optimization in fluid mechanics has been an active research field for several decades (Pironneau 1973, 1974). The goal of topology optimization is not only to find the optimal shape of fluidic channels, but also the optimal topology (or the optimal connectivity) of fluidic subdomains. Therefore, topology optimization is a more general optimization technique than shape optimization. Topology optimization for fluidic problems

was pioneered by Borrvall and Petersson for Stokes flow (Borrvall and Petersson 2003). Gersborg-Hansen et al. 2005 and Olesen et al. 2006 have extended fluidic topology optimization to low and moderate Reynolds number cases. The numerical methods which are used to calculate the fluid velocity and pressure are mainly the *finite element method* (FEM) (Gersborg-Hansen et al. 2005; Olesen et al. 2006; Evgrafov 2006; Gersborg-Hansen et al. 2006a; Aage et al. 2008), the *finite volume method* (FVM) (Gersborg-Hansen et al. 2006b) and the *finite difference method* (FDM) (Zadeh 2009).

2 Topology optimization of fluid channels

Topology optimization of flow channels with low and moderate Reynolds numbers using the FEM has been discussed in Gersborg-Hansen et al. (2005, 2006a), Olesen et al. (2006), Evgrafov (2006), and Aage et al. (2008). Usually, an incompressible Navier–Stokes equation is used to simulate the fluidic motion in channels. In addition, the governing equation is subject to an artificial friction force which is proportional to the fluid velocity \mathbf{u} . Based on the Darcy law, the friction force can be expressed as $\mathbf{f} = -\alpha \mathbf{u}$, where α is the impermeability of a porous medium (Guest and Prevost 2007). Therefore, one can modify an incompressible Navier–Stokes equation in the non-dimensional form as

$$\begin{aligned} Re(\mathbf{u} \cdot \nabla) \mathbf{u} + \nabla \cdot [-(\nabla \mathbf{u} + \nabla \mathbf{u}^T) + p \mathbf{I}] &= -\alpha \mathbf{u} \\ \nabla \cdot \mathbf{u} &= 0 \end{aligned} \quad (1)$$

where Re is the Reynolds number, \mathbf{u} is the fluid velocity, p is the fluid pressure and α depends on the optimiza-

Z. Liu (✉) · P. Zhang · M. Xuan · Y. Wu
State Key Laboratory of Applied Optics, Changchun Institute of
Optics, Fine Mechanics and Physics (CIOMP), Chinese Academy of
Sciences, 130033, Changchun, People's Republic of China
e-mail: liuzu@ciomp.ac.cn

Q. Gao
Graduate University of Chinese Academy of Sciences, Beijing,
People's Republic of China

tion design variable γ as (Borrvall and Petersson 2003; Gersborg-Hansen et al. 2005)

$$\alpha(\gamma) = \alpha_{\min} + (\alpha_{\max} - \alpha_{\min})(q(1 - \gamma))/(q + \gamma) \quad (2)$$

where α_{\min} and α_{\max} are the minimal and maximal values of α and q is a real and positive parameter used to adjust the convexity of the interpolation function in (2). The value of γ can vary between zero and one, where $\gamma = 0$ corresponds to an artificial solid domain and $\gamma = 1$ to a fluidic domain, respectively. In this paper, the parameters which are used to control the interpolation of an artificial material property are set to $\alpha_{\min} = 0$, $\alpha_{\max} = 10^3$ and $q = 0.1$. A commonly used objective function for fluidic optimization is the energy dissipation (Borrvall and Petersson 2003; Gersborg-Hansen et al. 2005, 2006a; Olesen et al. 2006; Evgrafov 2006; Aage et al. 2008)

$$\Phi(\mathbf{u}, \gamma) = \int_{\Omega} [\nabla \mathbf{u} \cdot (\nabla \mathbf{u} + \nabla \mathbf{u}^T) + \alpha(\gamma) \mathbf{u} \cdot \mathbf{u}] d\Omega \quad (3)$$

where Ω is the design domain. In this note, all the numerical examples have either prescribed velocities or pressure conditions on the boundary of the computational domain.

3 Flow rate equality constraints

In this note, we restrict our work on the optimization of two-dimensional flow channels with flow rate equality constraints on the specified boundaries. Topology optimization of fluid channels with flow rate equality constraints has been discussed by Gersborg-Hansen et al. (2005, 2006a) and Aage et al. (2008) using the method of moving asymptotes (MMA) (Svanberg 1987), where the equality constraints were approximated by using inequality constraints. For the equality constraint which is related to the forward physical problem, Liu and Korpink (2009) proposed the augmented Lagrangian method and have designed several compliant mechanisms with multiple equality displacement constraints. The Lagrange multiplier, which is related to the boundary condition of displacement, is calculated using the Lagrange multiplier method. In this note, the method proposed by Liu and Korpink (2009) is extended to the design of fluid channels with flow rate equality constraints

$$\int_{\Gamma_i} \mathbf{u} \cdot \mathbf{n} d\Gamma_i = \text{FR}_i * Q_{\text{in}}, \quad i = 1, \dots, m \quad (4)$$

where $\text{FR}_i \in [0, 1]$ is the ratio of the flow rate at boundary Γ_i , Q_{in} is the flow rate at the inlet and \mathbf{n} is the outward normal vector of the boundary Γ_i . The optimization prob-

lem can be expressed using the form of the augmented Lagrangian as

$$\begin{aligned} \text{Min : } L &= 2\Phi(\mathbf{u}, \gamma) + \sum_{i=1}^m \beta_i \left(\int_{\Gamma_i} \mathbf{u} \cdot \mathbf{n} d\Gamma_i - \text{FR}_i * Q_{\text{in}} \right) \\ &\quad + \sum_{i=1}^m \frac{\mu_i}{2} \left(\int_{\Gamma_i} \mathbf{u} \cdot \mathbf{n} d\Gamma_i - \text{FR}_i * Q_{\text{in}} \right)^2 \\ \text{s.t. } &\text{Re}(\mathbf{u} \cdot \nabla) \mathbf{u} + \nabla \cdot [-(\nabla \mathbf{u} + \nabla \mathbf{u}^T) + p \mathbf{I}] = -\alpha \mathbf{u} \\ &\nabla \cdot \mathbf{u} = 0 \\ &\int_{\Omega} \gamma d\Omega < \text{Vol}_{\Omega} * \text{Vol}^*, \quad 0 \leq \gamma \leq 1 \end{aligned} \quad (5)$$

where β_i and μ_i are the Lagrange multipliers and penalty coefficients required to implement the equality constraints of flow rate on the boundary of Γ_i , $\text{Vol}^* \in [0, 1]$ is a scalar and Vol_{Ω} is the area of the whole design domain. Based on the finite element theory, the physical meaning of the Lagrange multiplier β_i is the normal stress which acts on the corresponding boundary Γ_i in order to fulfill a specified flow rate.

For the sensitivity analysis of the optimization problem in (5), the adjoint method is typically used for topology optimization where the number of design variables is much higher than the number of design criteria (Gersborg-Hansen et al. 2005). The discretized form of the objective function in (5) can be expressed as

$$\begin{aligned} L &= 2\Phi(\mathbf{U}, \gamma) + \lambda_{\beta}^T R(\mathbf{U}, \gamma) + \lambda_{\mu}^T R(\mathbf{U}, \gamma) \\ &\quad + \sum_{i=1}^m \left(\beta_i (l_i^T \mathbf{U} - \text{FR}_i * Q_{\text{in}}) \right. \\ &\quad \left. + \frac{\mu_i}{2} (l_i^T \mathbf{U} - \text{FR}_i * Q_{\text{in}})^2 \right) \end{aligned} \quad (6)$$

where \mathbf{U} is the combined vector of velocity \mathbf{u} and pressure p , $R(\mathbf{U}, \gamma) = 0$ is the discretized Navier–Stokes equation in residual form, the λ_{β} and λ_{μ} are the adjoint vectors and l^T is the vector with a value of 1 at the degrees of freedom corresponding to the boundary with the flow rate constraint. The first-order derivative of the objective in (6) with respect to the design variable γ is

$$\begin{aligned} \frac{dL}{d\gamma} &= 2 \frac{\partial \Phi}{\partial \mathbf{U}} \frac{d\mathbf{U}}{d\gamma} + 2 \frac{\partial \Phi}{\partial \gamma} + \lambda_{\beta}^T \left(\frac{\partial R}{\partial \mathbf{U}} \frac{d\mathbf{U}}{d\gamma} + \frac{\partial R}{\partial \gamma} \right) \\ &\quad + \lambda_{\mu}^T \left(\frac{\partial R}{\partial \mathbf{U}} \frac{d\mathbf{U}}{d\gamma} + \frac{\partial R}{\partial \gamma} \right) + \sum_{i=1}^m \left(\beta_i l_i^T + \theta_i l_i^T \right) \frac{d\mathbf{U}}{d\gamma} \end{aligned} \quad (7)$$

where $\theta_i = \mu_i (l_i^T \mathbf{U} - \text{FR}_i * Q_{\text{in}})$ is the residual of the flow rate constraint on the boundary Γ_i . The discretized residual

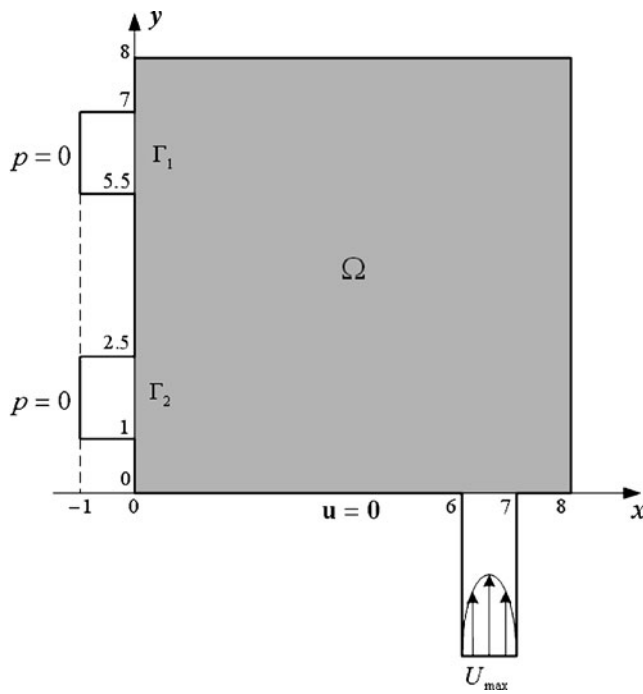


Fig. 1 The design domain Ω (gray square) and the computational domain for the optimization of splitter channel. All the boundaries on the computational domain are no-slip ($\mathbf{u} = 0$) unless otherwise marked

form of Navier–Stokes equation $R(\mathbf{U}, \gamma) = 0$ is assumed to be zero for the current design variable γ by solving (1) with boundary conditions

$$\mathbf{u} = \mathbf{u}_{\text{in}} \text{ on } \Gamma_{\text{in}}, \quad \mathbf{u} = 0 \text{ on } \Gamma_{\partial\Omega}, \quad p = 0 \text{ on } \Gamma_{\text{out}} \quad (8)$$

Therefore, the terms $\frac{\partial \lambda_\beta}{\partial \gamma} R$ and $\frac{\partial \lambda_\mu}{\partial \gamma} R$ are zero. In (6), the Lagrange multipliers β_i and the penalty coefficients μ_i are treated as independent variables. Therefore $\frac{\partial \beta_i}{\partial \gamma}$ and $\frac{\partial \mu_i}{\partial \gamma}$ are zero too. Equation (7) can be simplified as

$$\frac{dL}{d\gamma} = \left(\frac{\partial \Phi}{\partial \gamma} + \lambda_\beta^T \frac{\partial R}{\partial \gamma} \right) + \left(\frac{\partial \Phi}{\partial \gamma} + \lambda_\mu^T \frac{\partial R}{\partial \gamma} \right) \quad (9)$$

Fig. 2 a The distribution of design variable γ for the optimized splitter channels with design parameters $\text{FR}_1 = \text{FR}_2 = 1/2$, $\text{Vol}^* = 0.4$ and $\text{Re} = 1$; b) The optimization history of normalized energy dissipation and the ratio of flow rate



by solving the following two adjoint equations

$$\begin{aligned} \lambda_\beta^T \frac{\partial R}{\partial \mathbf{U}} &= -\frac{\partial \Phi}{\partial \mathbf{U}} - \sum_{i=1}^m \beta_i l_i^T \\ \lambda_\mu^T \frac{\partial R}{\partial \mathbf{U}} &= -\frac{\partial \Phi}{\partial \mathbf{U}} - \sum_{i=1}^m \theta_i l_i^T \end{aligned} \quad (10)$$

In (5), the energy dissipation $\Phi(\mathbf{u}, \gamma)$ is multiplied by two. In (6), the residual form of Navier–Stokes equation $R(U, \gamma)$ is included twice with different adjoint vectors. This allows us to calculate the adjoint vectors λ_β and λ_μ separately in (10).

4 Discussion

4.1 Computational cost associated with optimization

For the optimization problem in (5), the computational cost for each iteration is mainly caused by (a) solving the vector \mathbf{U} , the Lagrange multiplier β_i and adjoint vectors λ_β and λ_μ ; (b) calculating the first-order sensitivity $dL/d\gamma$; and (c) updating the design variables γ through the MMA algorithm. The nonlinear Navier–Stokes equation is solved in order to obtain a converged solution of \mathbf{U} based on the current value of design variable γ . Here the vector \mathbf{U} , which is called the solution of the forward problem, will be used later when solving the adjoint vectors and the Lagrange multipliers. The term $\partial R/\partial \mathbf{U}$ in adjoint equation (10) is the Jacobian matrix of the residual equation $R(\mathbf{U}, \gamma) = 0$, where the matrix $\partial R/\partial \mathbf{U}$ can be evaluated using the converged solution of the forward problem. Therefore the two adjoint equations are both linear equations, allowing for the efficient solution of the adjoint vectors λ_β and λ_μ (Gersborg-Hansen et al. 2005). For the Lagrange multiplier β_i , a suitable value can be chosen at the beginning

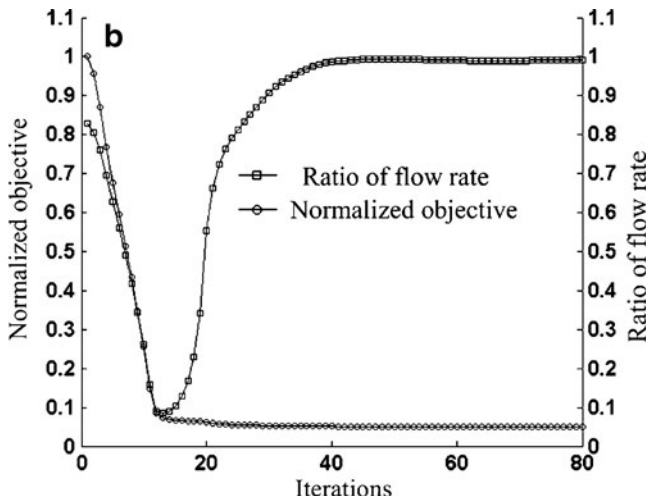
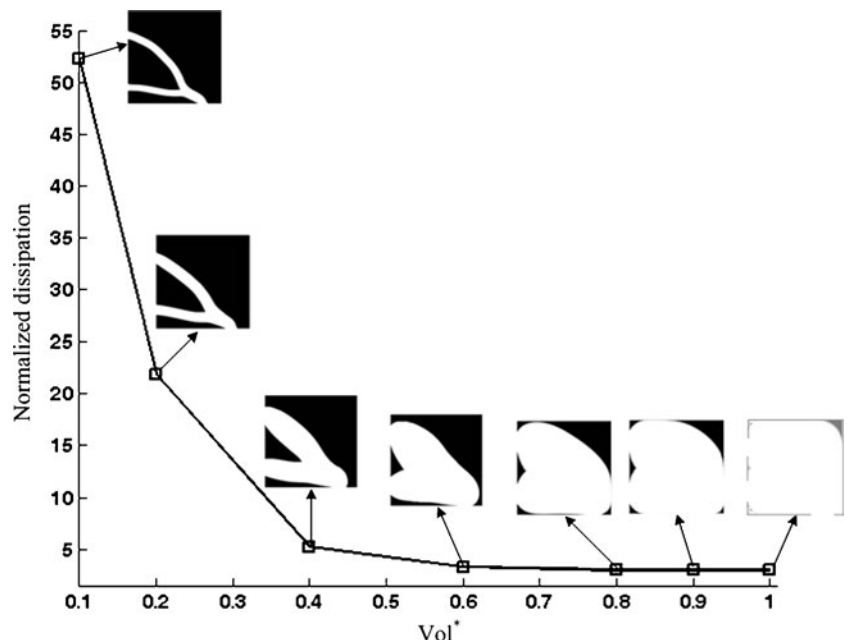


Fig. 3 The optimized results of splitter channels where the value of Vol^* is swept from 0.1 to 1.0. The other optimization parameters are same as the example shown in Fig. 2. The energy dissipation for the case that $\text{Vol}^* = 1.0$ is normalized as 1.0



of the optimization, and the value of the Lagrange multiplier can be updated based on certain rules (Bertsekas 1996). Alternatively, the Lagrange multiplier can be calculated by solving the Navier–Stokes equation with the flow rate boundary conditions in (4) (Formaggia et al. 2002). In order to implement optimization iteration efficiently, an approximate solution of the Lagrange multiplier β_i can be obtained by using a linearized Navier–Stokes equation, where the linearization points are the converged solution of the forward problem. Compared with the MMA algorithm, the additional computational cost for evaluating the first-order sensitivity vector is mainly for solving a linearized equation in order to calculate the Lagrange multipliers β_i . However, the optimization problem is simplified with only one inequality constraint, which is used to limit channel areas. At the same time, there is no need to use an inequality constraint to approximate an equality constraint by tuning the residual of constraint carefully.

4.2 Quadratic penalty term

For the optimization problem in (5), the quadratic penalty term is used to improve the convergence of equality constraints. However, it is known that too large a value of the penalty coefficient μ will result in an ill-conditioned problem. One has to choose a reasonable value of μ (Nocedal and Wright 1999). In (9), the first-order sensitivity is separated into two parts with the second part being related to the quadratic penalty term. In order to maintain the stability of optimization for a relatively large value of the penalty

coefficient μ , the cut-off sensitivity based on the first-order sensitivity in (9) is used as

$$\frac{dL}{d\gamma} = \left(\frac{\partial \Phi}{\partial \gamma} + \lambda_\beta^T \frac{\partial R}{\partial \gamma} \right) + \min \left(0, \frac{\partial \Phi}{\partial \gamma} + \lambda_\mu^T \frac{\partial R}{\partial \gamma} \right) \quad (11)$$

4.3 Numerical implementation of the optimization problem

Optimization of fluidic channels with flow rate equality constraints is implemented using the commercial finite element software Comsol (<http://www.comsol.com>). The non-linear Navier–Stokes equation is solved by using a linear Lagrange finite element for both the velocity and pressure fields. Given that the velocity and pressure interpolation are of the same order, usually a pressure stabilization,

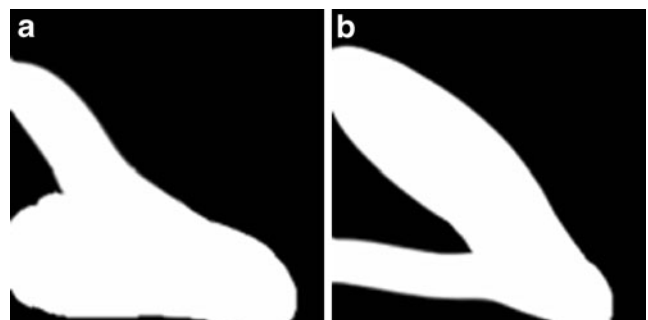
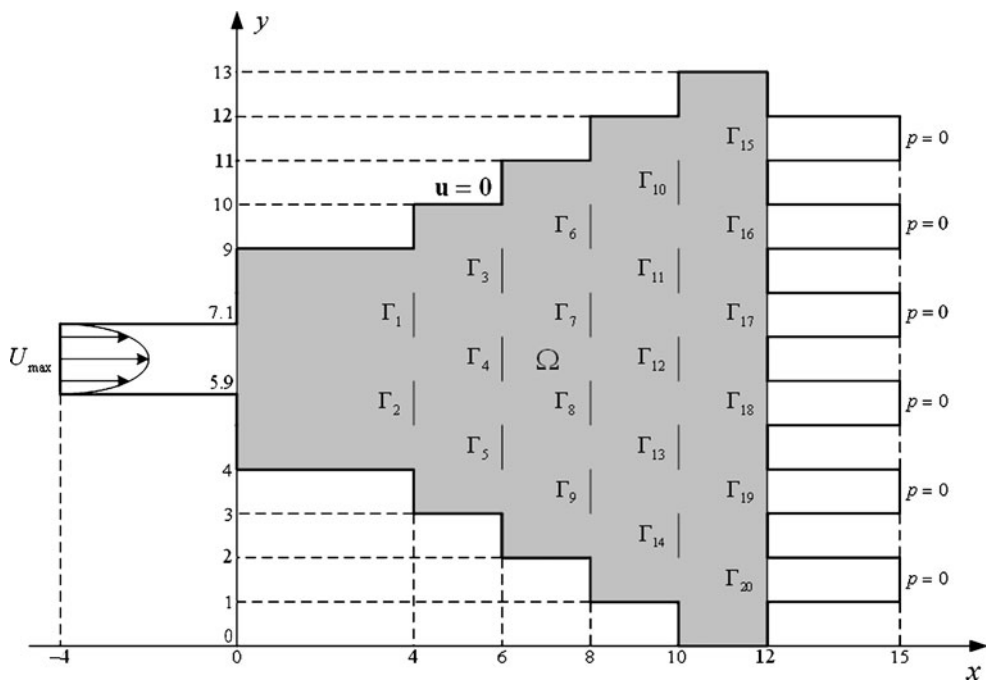


Fig. 4 The distribution of design variable γ for the optimized splitter channels with design parameters $\text{Vol}^* = 0.4$ and $\text{Re} = 1$. The flow rate on the specified boundaries are: **a** $\text{FR}_1 = 1/4, \text{FR}_2 = 3/4$; **b** $\text{FR}_1 = 3/4, \text{FR}_2 = 1/4$

Fig. 5 The design domain Ω (gray part) and the computational domain for the optimization of flow distributor. All the boundaries on the frame of computational domain are no-slip ($\mathbf{u} = 0$) unless otherwise marked



e.g. pressure-stabilizing/Petrov–Galerkin (PSPG) method, would be necessary. In this note, the numerical stability is maintained by using the Galerkin least-square method, and the design domain is discretized with a sufficient number of rectangular elements (Hauke and Hughes 1994). The Lagrange multiplier β_i , which is related to the boundary condition of the flow rate, is calculated by using the *weak constraint* function in Comsol. One can refer to Olesen et al. (2006) for a detailed numerical implementation of the adjoint sensitivity analysis in Comsol. The optimization iterations are stopped when the residual of the flow rate

$$\left| \int_{\Gamma_i} \mathbf{u} \cdot \mathbf{n} \, d\Gamma_i / Q_{\text{in}} - \text{FR}_i \right| < 1e-3 \quad (12)$$

and the change of normalized energy dissipation between two consecutive iterations

$$|\Phi_{k+1} - \Phi_k| < 1e-3 \quad (13)$$

5 Numerical examples

5.1 Splitter with two outlets

The flow splitter has been used as a functional unit to control the flow rate at different outlets in order to separate micro particles (Takagi et al. 2005). In this example, the layout of flow channels with specified flow rates on two

outlets is optimized based on the optimization problem in (5). The upper bound for the constraint of flow channel areas is chosen as $\text{Vol}^* = 0.4$ and the Reynolds number $\text{Re} = 1$. The initial value of the penalty parameter μ is 1 and the maximum value is limited to 100. The computational domain is shown in Fig. 1 where the design domain is shown as the gray subdomain. The flow rate constraints are specified on the two boundaries Γ_1 and Γ_2 , which connect the design domain and outlet tubes. The design domain is discretized by 160×160 rectangular elements. Figure 2a shows an optimized result where the flow rate of two outlets is $\text{FR}_1 = \text{FR}_2 = 0.5$. Figure 2b shows the optimization history about the normalized objective function Φ and the ratio of flow rates ($\int_{\Gamma_1} \mathbf{u} \cdot \mathbf{n} d\Gamma_1 / \int_{\Gamma_2} \mathbf{u} \cdot \mathbf{n} d\Gamma_2$) on two

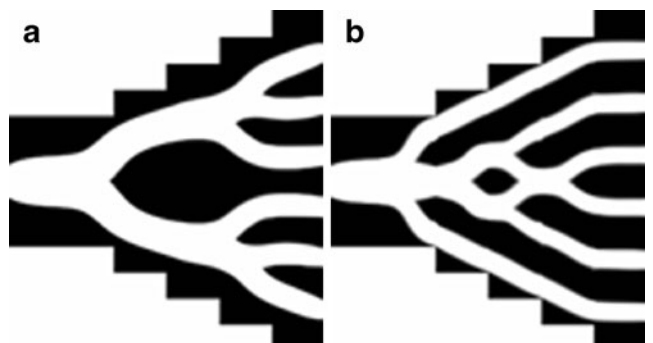


Fig. 6 The optimized distributor with design parameters $\text{Vol}^* = 0.4$, $\text{Re} = 1$. The flow rate on the specified boundaries are: **a** $\text{FR}_{15} \sim \text{FR}_{20} = 1/6$; **b** $\text{FR}_1 \sim \text{FR}_{14} = 0$, $\text{FR}_{15} \sim \text{FR}_{20} = 1/6$

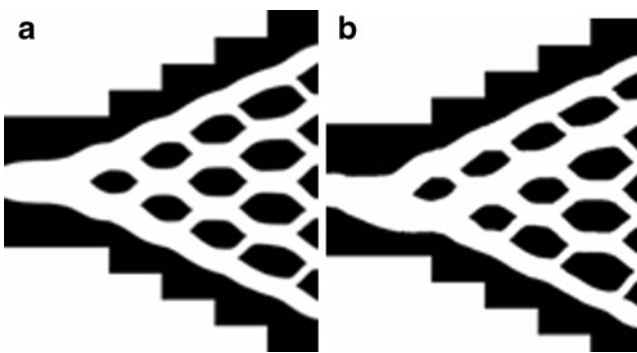


Fig. 7 The optimized channel with design parameters $\text{Vol}^* = 0.4$, $\text{Re} = 1$. The flow rate on the specified boundaries are: **a** $\text{FR}_1 = \text{FR}_2 = 1/2$, $\text{FR}_3 \sim \text{FR}_5 = 1/3$, $\text{FR}_6 \sim \text{FR}_9 = 1/4$, $\text{FR}_{10} \sim \text{FR}_{14} = 1/5$, $\text{FR}_{15} \sim \text{FR}_{20} = 1/6$; **b** $\text{FR}_1 = 1/3$, $\text{FR}_2 = 2/3$, $\text{FR}_3 = 1/4$, $\text{FR}_4 = 1/2$, $\text{FR}_5 = 1/4$, $\text{FR}_6 = 1/5$, $\text{FR}_7 = 2/5$, $\text{FR}_8 = \text{FR}_9 = 1/5$, $\text{FR}_{10} = 1/6$, $\text{FR}_{11} = 1/3$, $\text{FR}_{12} = \text{FR}_{13} = \text{FR}_{14} = 1/6$, $\text{FR}_{15} = 1/7$, $\text{FR}_{16} = 2/7$, $\text{FR}_{17} = \text{FR}_{18} = \text{FR}_{19} = \text{FR}_{20} = 1/7$

outlets. For the optimization problem in (5), an inequality constraint is used to control the area of fluid channels. Figure 3 shows the optimized geometries of fluid channels where the value of Vol^* is swept from 0.1 to 1.0 while the other optimization parameters are the same as the example used in Fig. 2a. The flow rate constraints are all satisfied for these results, and the optimized channels look more like the channels used in microfluidic devices when a small value of Vol^* is used. Figure 4 shows the optimized results where the flow rates on the two outlets are $\{\text{FR}_1 = 1/4, \text{FR}_2 = 3/4\}$ and $\{\text{FR}_1 = 3/4, \text{FR}_2 = 1/4\}$, respectively.

5.2 Flow distributor with multiple flow rate constraints

The flow distributor has been used as a functional unit to distribute a certain volume of fluid over a specified subdomain in microfluidics (Vangelooven et al. 2010). In this note, a radial interconnecting distributor is designed with specified flow rates at different positions. The design domain is shown in Fig. 5 where the flow rates on 20 outlets need to be controlled accurately. The upper bound for the constraint of flow channel areas is chosen as $\text{Vol}^* = 0.4$ and the design domain is discretized by 160,000 rectangular elements. Figure 6a shows the optimized distributor where only outlets $\Gamma_{15} \sim \Gamma_{20}$ are constrained as $\text{FR}_{15} \sim \text{FR}_{20} = 1/6$. Figure 6b shows the design of the distributor where $\Gamma_1 \sim \Gamma_{14}$ inside the design domain are constrained to have a zero flow rate ($\text{FR}_1 \sim \text{FR}_{14} = 0$) and outlets $\Gamma_{15} \sim \Gamma_{20}$ are constrained as $\text{FR}_{15} \sim \text{FR}_{20} = 1/6$. Figure 7a and b show the optimized results where the flow rates on 20 outlets are specified with a symmetrical and unsymmetrical distribution, respectively.

Acknowledgments The authors thank the reviewers for their valuable comments. This work was supported by the China National Science fund (No. 50975272), the China National High Technology Research and Development program (863 program) (No. 2007 AA 042102) and SKLАО open fund in CIOMP. Prof. Krister Svanberg is gratefully acknowledged for his free Matlab code of MMA.

References

- Aage N, Poulsen TH, Gersborg-Hansen A, Bendsoe MP, Sigmund O (2008) Topology optimization of large scale stokes flow problems. *Struct Multidiscipl Optim* 35:175–180
- Andreasen CS, Gersborg AR, Sigmund O (2008) Topology optimization of microfluidic mixers. *Int J Numer Methods Fluids* 61:498–513
- Bertsekas DP (1996) Constrained optimization and Lagrange multiplier methods. Athena Scientific
- Borrvall T, Petersson J (2003) Topology optimization of fluids in stokes flow. *Int J Numer Methods Fluids* 41:77–107
- Deng Y, Liu Z, Zhang P, Wu Y, Korvink JG (2010) Optimization of no-moving-part fluidic resistance microvalves with low Reynolds number. In: The 23th IEEE MEMS conference, pp 67–70
- Evgrafov A (2006) Topology optimization of slightly compressible fluids. *ZAMM* 86:46–62
- Formaggia L, Gerbeau JF, Nobile F, Quarteroni A (2002) Numerical treatment of defective boundary conditions for the Navier–Stokes equations. *SIAM J Numer Anal* 40:376–401
- Gersborg-Hansen A, Sigmund O, Haber RB (2005) Topology optimization of channel flow problems. *Struct Multidiscipl Optim* 30:181–192
- Gersborg-Hansen A, Berggren M, Dammann B (2006a) Topology optimization of mass distribution problems in Stokes flow. In: IUTAM symposium on topological design optimization of structures, machines and materials. Springer, Netherlands, pp 356–374
- Gersborg-Hansen A, Bendsoe MP, Sigmund O (2006b) Topology optimization of heat conduction problems using the finite volume method. *Struct Multidisc Optim* 31:251–259
- Guest JK, Prevost JH (2007) Design of maximum permeability material structures. *Comput Methods Appl Mech Eng* 196:1006–1017
- Hauke G, Hughes TJR (1994) A unified approach to compressible and incompressible flows. *Comput Methods Appl Mech Eng* 113:389–395
- Liu Z, Korvink JG (2009) Using artificial reaction force to design compliant mechanism with multiple equality displacement constraints. *Finite Elem Anal Des* 45:555–568
- Nocedal J, Wright SJ (1999) Numerical optimization. Springer
- Okkels F, Bruus H (2007) Scaling behavior of optimally structured catalytic microfluidic reactors. *Phys Rev E* 75:1–4
- Okkels F, Olesen LH, Bruus H (2005) Application of topology optimization in the design of micro- and nanofluidic systems. *NSTI-Nanotech* 1:575–578
- Olesen LH, Okkels F, Bruus H (2006) A high-level programming-language implementation of topology optimization applied to steady-state Navier–Stokes flow. *Int J Numer Methods Eng* 65:975–1001
- Pironneau O (1973) On optimum profiles in stokes flow. *J Fluid Mech* 59:117–128
- Pironneau O (1974) On optimum design in fluid mechanics. *J Fluid Mech* 64:97–110

- Svanberg K (1987) The method of moving asymptotes: a new method for structural optimization. *Int J Numer Methods Eng* 24: 359–373
- Takagi J, Yamada M, Yasuda M, Seki M (2005) Continuous particle separation in a microchannel having asymmetrically arranged multiple branches. *Lab Chip* 5:778–784
- Vangelooen J, Malsche WD, Beeck JOD, Eghbali H, Gardeniers H, Desmet G (2010) Design and evaluation of flow distributors for microfabricated pillar array columns. *Lab Chip* 10:349–356
- Zadeh KS (2009) Multi-objective optimization in variably saturated fluid flow. *J Comput Appl Math* 223:801–819